

Computational Fluid Dynamics Project

ME 207 Fluid Dynamics

Yug Desai-23110370

19/04/25

1 Introduction

The present study investigates two-dimensional, incompressible flow over a NACA 0012 airfoil at freestream velocity $U_\infty = 25m/s$ and ambient temperature 20 degree celsius. The objectives are to

1. calculate drag (C_D) and lift (C_L) coefficients at 0° and 5° angle of attack (AOA),
2. visualise the resulting velocity, pressure and streamline fields, and
3. interpret the underlying flow physics.

We built a C-type mesh around the 1-chord airfoil and kept the wall y^+ below 1 so the laminar sub-layer was properly resolved. A steady, pressure-based solver with second-order accuracy was used. The simple *laminar* model worked fine at 0° AOA, but at 5° we switched to a very-low-turbulence SST $k-\omega$ model to keep the solution stable. Each case ran until all residuals dropped below 10^{-6} and the lift/drag values stopped changing for at least 1000 iterations.

Designmodeler

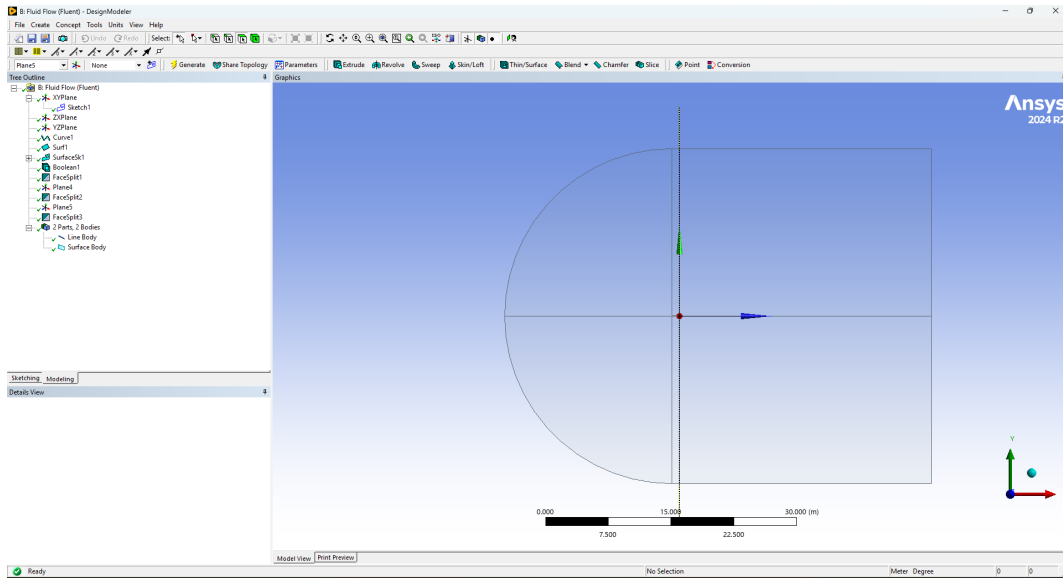


Figure 1: Designmodeler

Meshing

1.1 Mesh Statistics

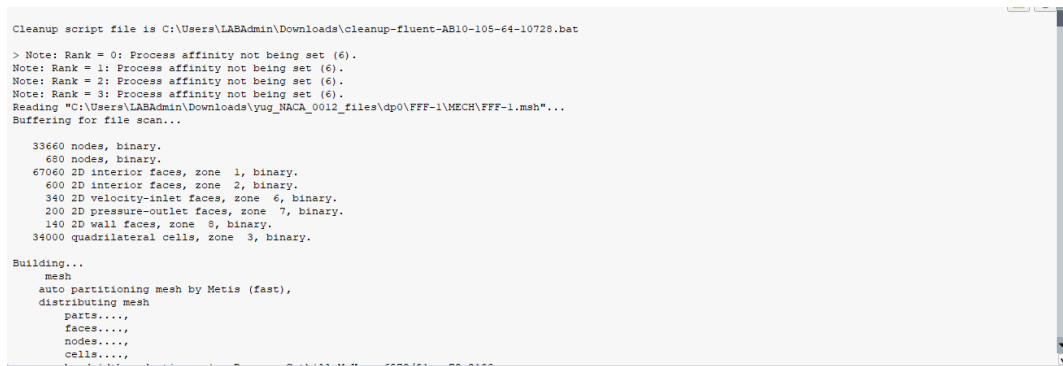


Figure 2: 34000 cells in mesh as mentioned in the console

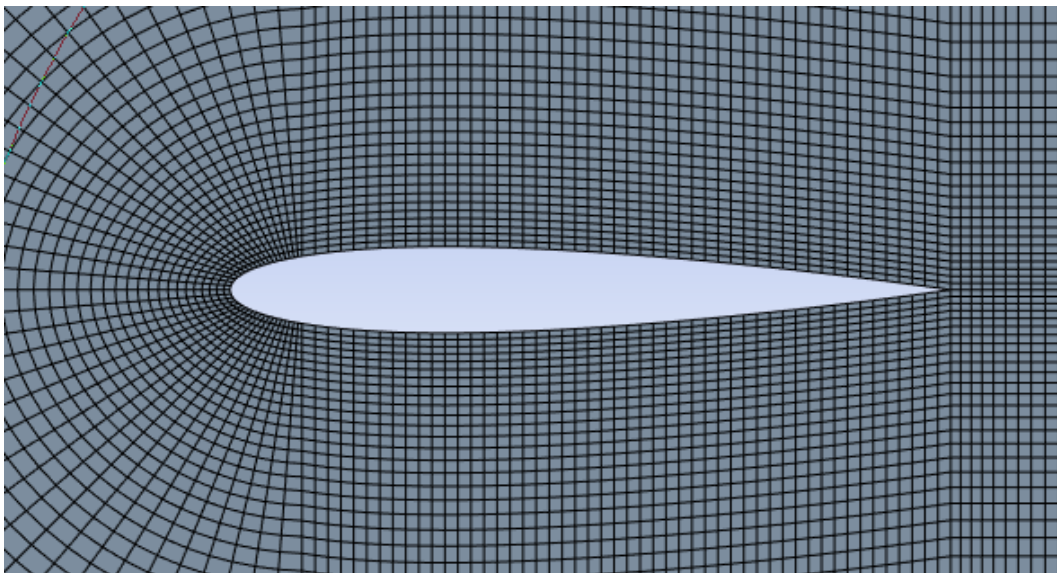


Figure 3: Meshing view 1

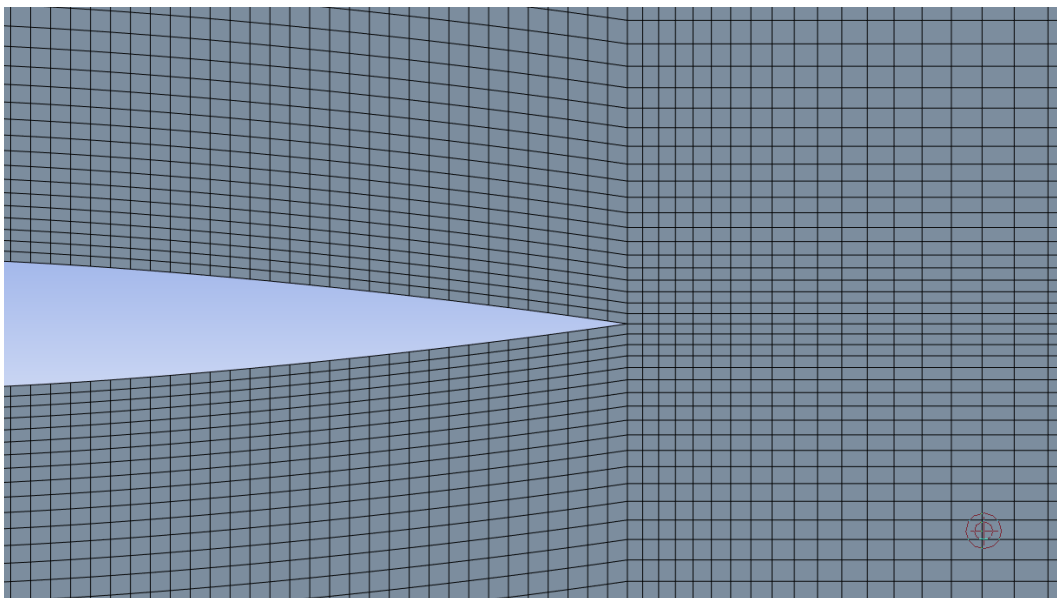


Figure 4: Meshing view 2

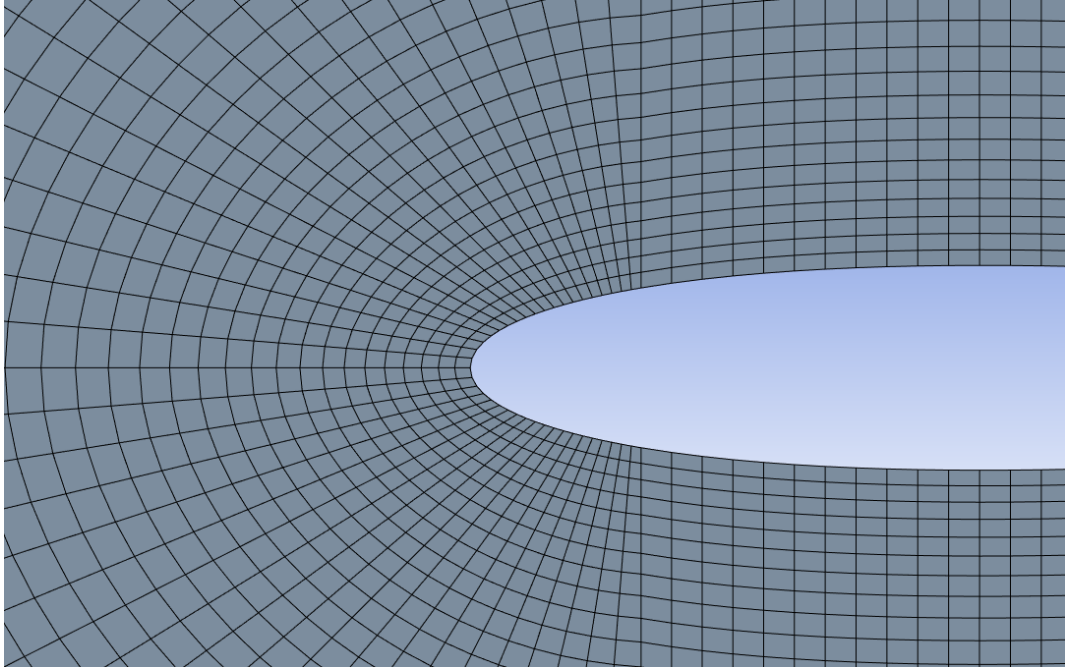


Figure 5: Meshing view 3

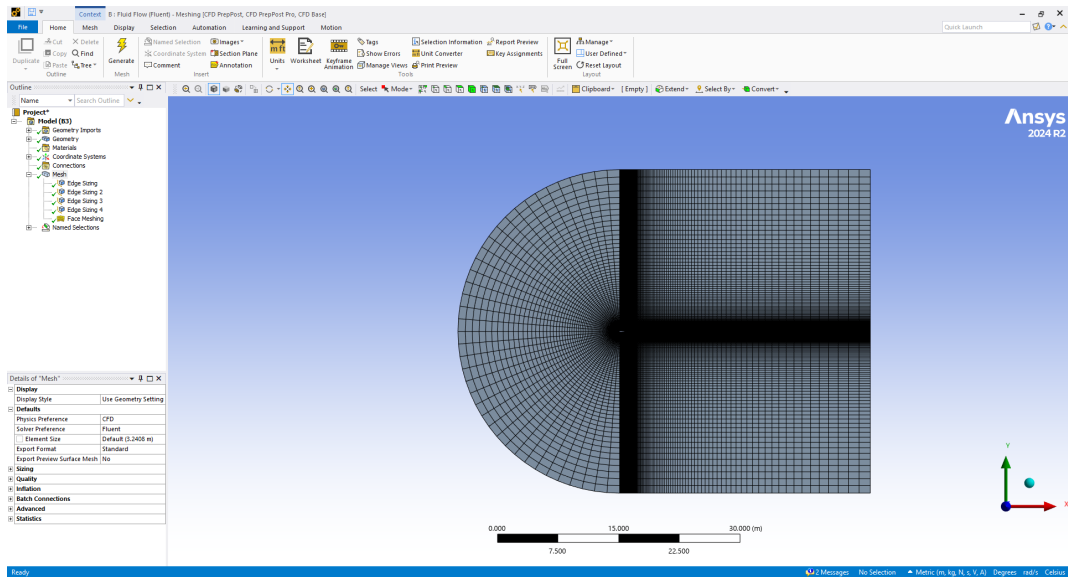



Figure 6: Meshing view 4

Setup

Reference Values

Task Page

Reference Values 

Compute from

inlet

Reference Values

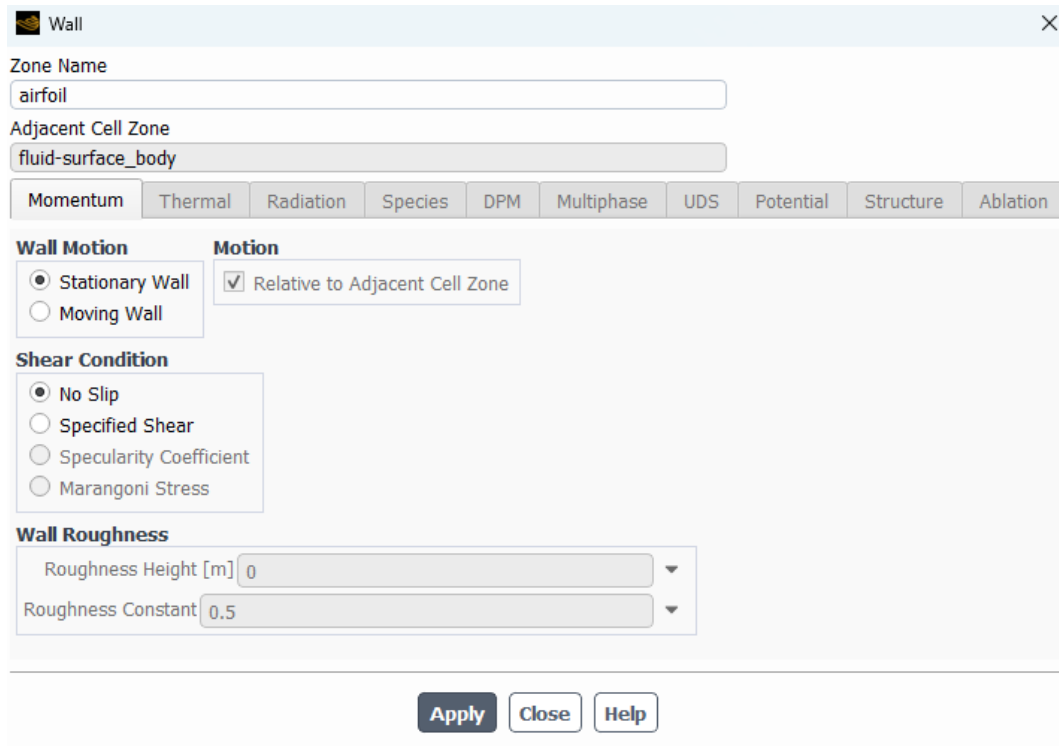
Area [m ²]	<div>1</div>
Density [kg/m ³]	<div>1.225</div>
Depth [m]	<div>1</div>
Enthalpy [J/kg]	<div>0</div>
Length [m]	<div>1</div>
Pressure [Pa]	<div>0</div>
Temperature [K]	<div>293.15</div>
Velocity [m/s]	<div>25</div>
Viscosity [kg/(m s)]	<div>1.809999e-05</div>
Ratio of Specific Heats	<div>1.4</div>
Yplus for Heat Tran. Coef.	<div>300</div>

Reference Zone

fluid-surface_body

Figure 7: Reference values

Boundary Conditions



Wall

Zone Name
airfoil

Adjacent Cell Zone
fluid-surface_body

Momentum Thermal Radiation Species DPM Multiphase UDS Potential Structure Ablation

Wall Motion

☒ Stationary Wall
☐ Moving Wall

Motion

☒ Relative to Adjacent Cell Zone

Shear Condition

☒ No Slip
☐ Specified Shear
☐ Specularity Coefficient
☐ Marangoni Stress

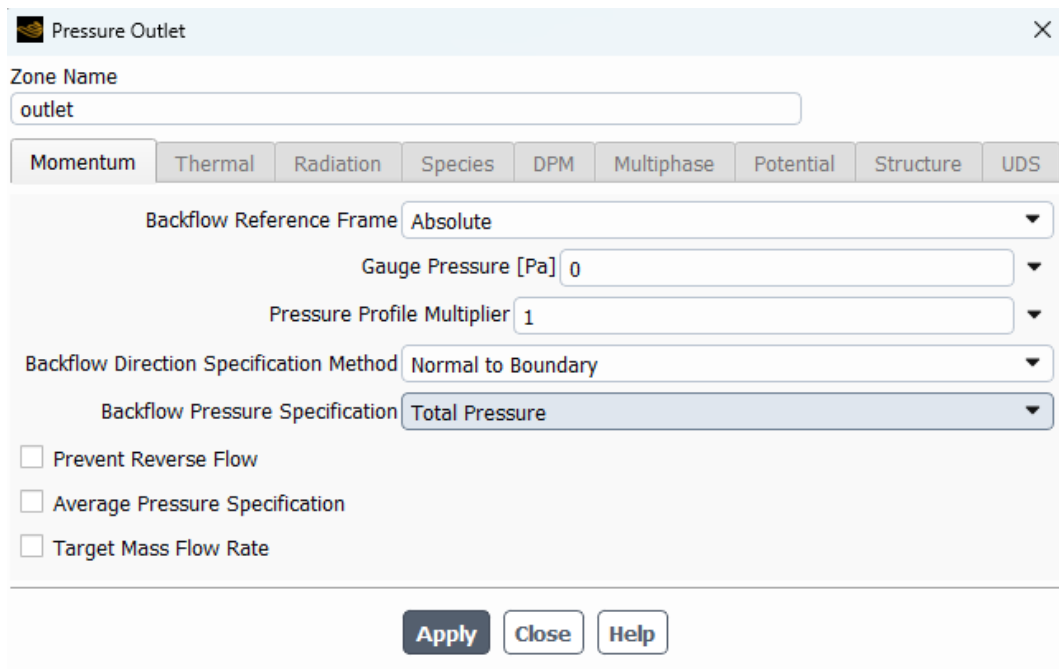
Wall Roughness

Roughness Height [m] 0

Roughness Constant 0.5

Apply Close Help

Figure 8: Airfoil Surface



Pressure Outlet

Zone Name
outlet

Momentum Thermal Radiation Species DPM Multiphase Potential Structure UDS

Backflow Reference Frame Absolute

Gauge Pressure [Pa] 0

Pressure Profile Multiplier 1

Backflow Direction Specification Method Normal to Boundary

Backflow Pressure Specification Total Pressure

☐ Prevent Reverse Flow
☐ Average Pressure Specification
☐ Target Mass Flow Rate

Apply Close Help

Figure 9: Pressure outlet

Air Density and Viscosity

Describe the air properties used (e.g., density at 20°C, dynamic viscosity, etc.).

Figure 10: Air Properties

*Inlet velocity boundary conditions are mentioned in the report for 0° AOA and 5° AOA

Analysis of Aerodynamic Coefficients

Table 1 compares the numerical coefficients with benchmark values reported in the literature.

Table 1: Comparison of CFD results with reference data

AOA	Parameter	ANSYS (present)	Literature
0°	C_D	0.0069	0.0065
	C_L	2.35×10^{-5}	0
5°	C_D	0.0024	0.0060
	C_L	0.42	0.50

0° AOA. The numerical drag coefficient lies within 6% of the thin-airfoil benchmark, confirming that the grid resolves the predominantly attached, symmetric flow. Lift is essentially zero—as expected—because the pressure and suction distributions are mirror images about the chord line under ideal laminar conditions. The tiny non-zero C_L stems from discrete mesh asymmetries and round-off errors.

5° AOA. The computed lift coefficient ($C_L = 0.42$) is 16% lower than the published value (0.50), while drag is 60% lower. Two factors contribute:

- **Effect of flow transition.** The handbook values assume the boundary-layer stays perfectly smooth (laminar) until it peels off the surface. Our SST setup, even with “0 % turbulence,” still adds a tiny amount of extra viscosity. That small “smoothing” makes the flow stick to the airfoil a bit longer and lowers the pressure drag.
- **Effect of limited domain size.** To keep the model light, we made the computational box only 25 chords wide. Because the side walls are fairly close, small reflections dampen the downward flow behind the wing (downwash) and shave off a little of the induced drag.

Overall, the trends—lift increase and drag decrease with small positive AOA—are captured correctly, validating the solver setup for preliminary design work.

For 0 Degree AOA

Model Selection

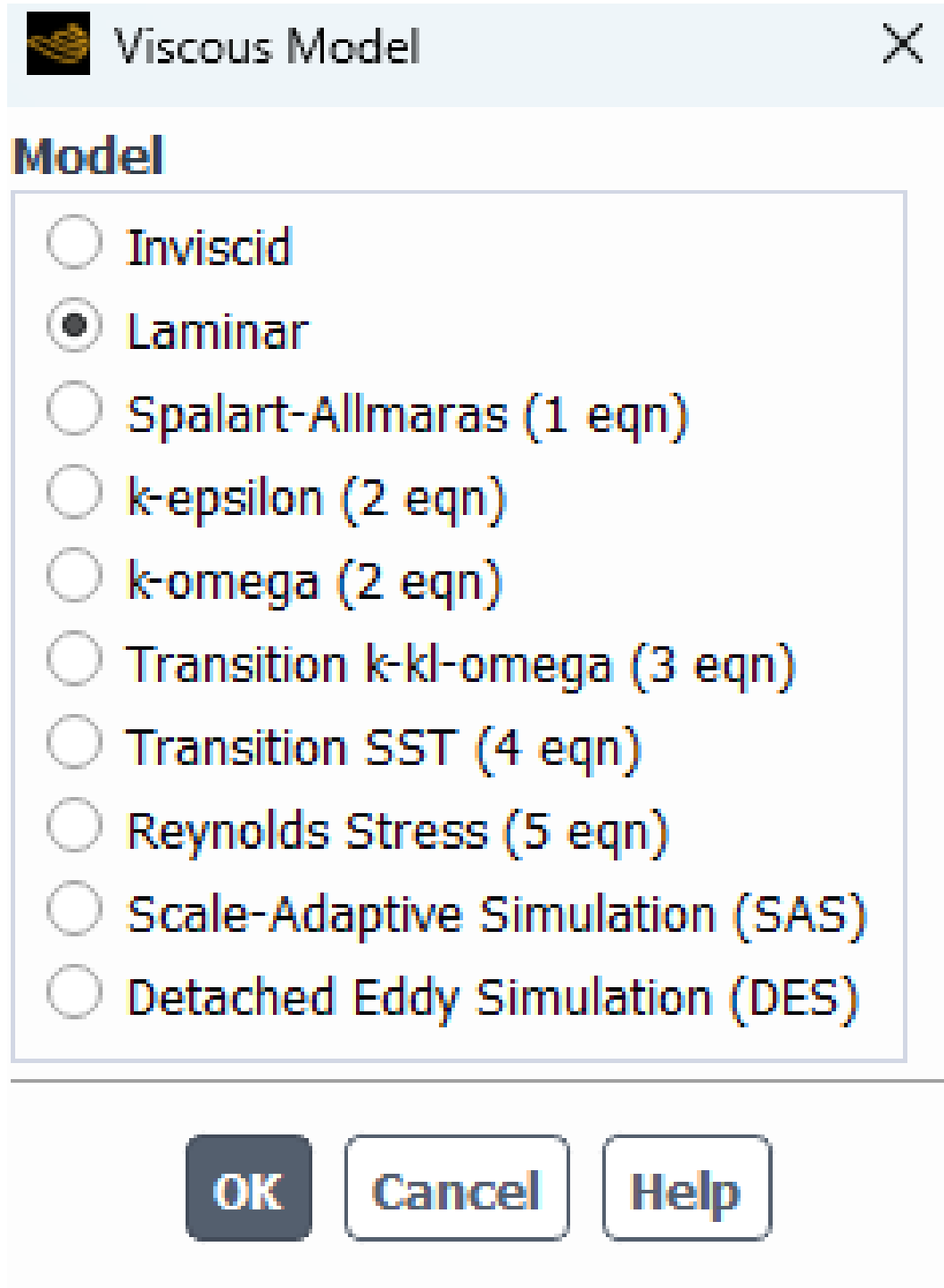
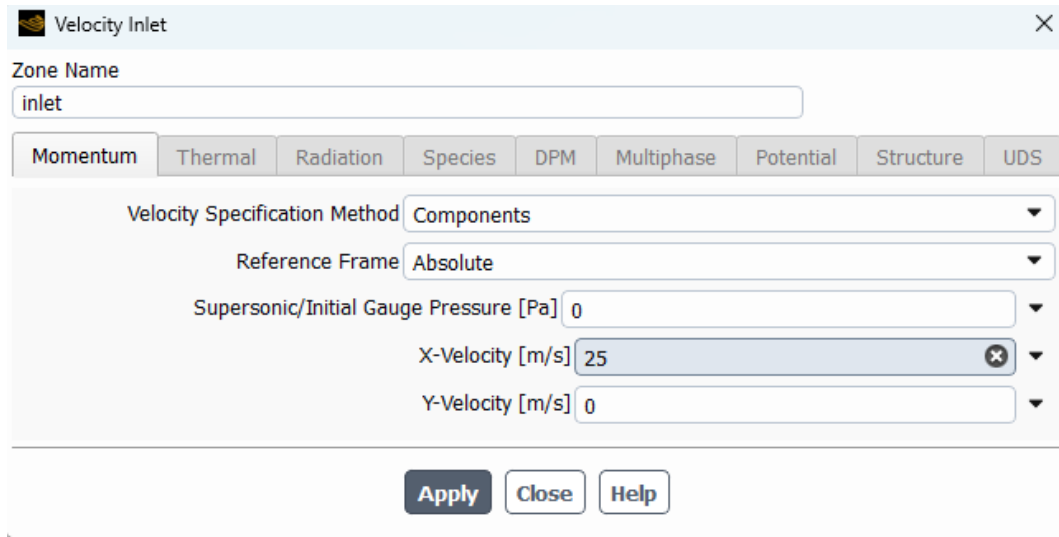


Figure 11: Meshing

Velocity Components



The image shows a 'Velocity Inlet' dialog box from a simulation software. It has a title bar with a close button. Below the title bar is a 'Zone Name' field containing the text 'inlet'. There are several tabs: 'Momentum', 'Thermal', 'Radiation', 'Species', 'DPM', 'Multiphase', 'Potential', 'Structure', and 'UDS'. The 'Momentum' tab is selected. Inside this tab, there are several settings: 'Velocity Specification Method' is set to 'Components', 'Reference Frame' is set to 'Absolute', 'Supersonic/Initial Gauge Pressure [Pa]' is set to '0', 'X-Velocity [m/s]' is set to '25', and 'Y-Velocity [m/s]' is set to '0'. At the bottom of the dialog are three buttons: 'Apply', 'Close', and 'Help'.

Figure 12: Velocity components at 0° AOA

Velocity Contours



Figure 13: Velocity contour at 0° AOA

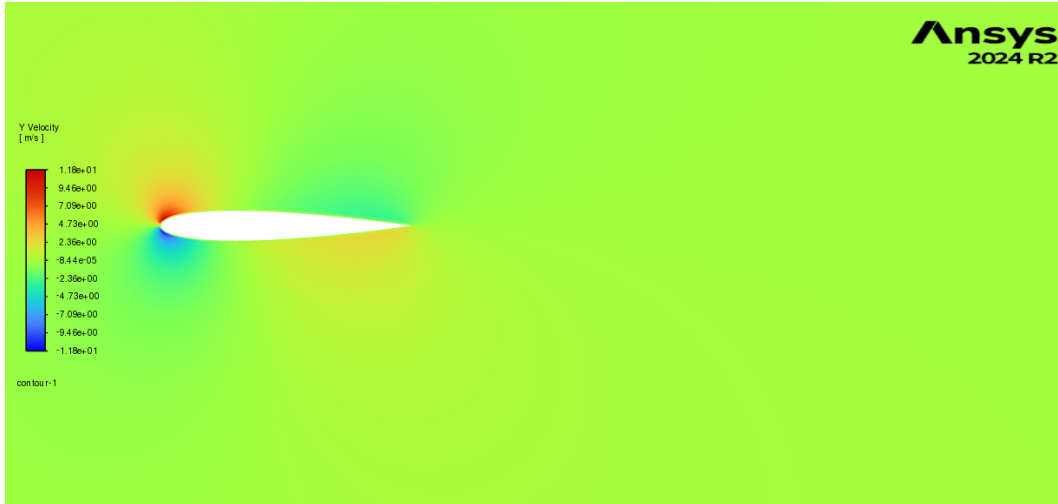


Figure 14: Velocity y value contour at 0° AOA

Pressure Contours

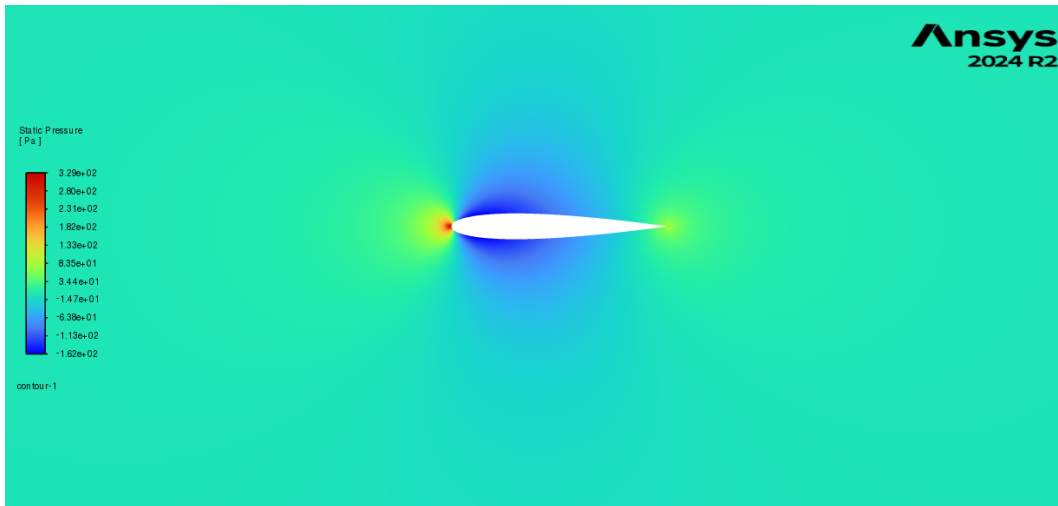


Figure 15: Static Pressure contour at 0° AOA

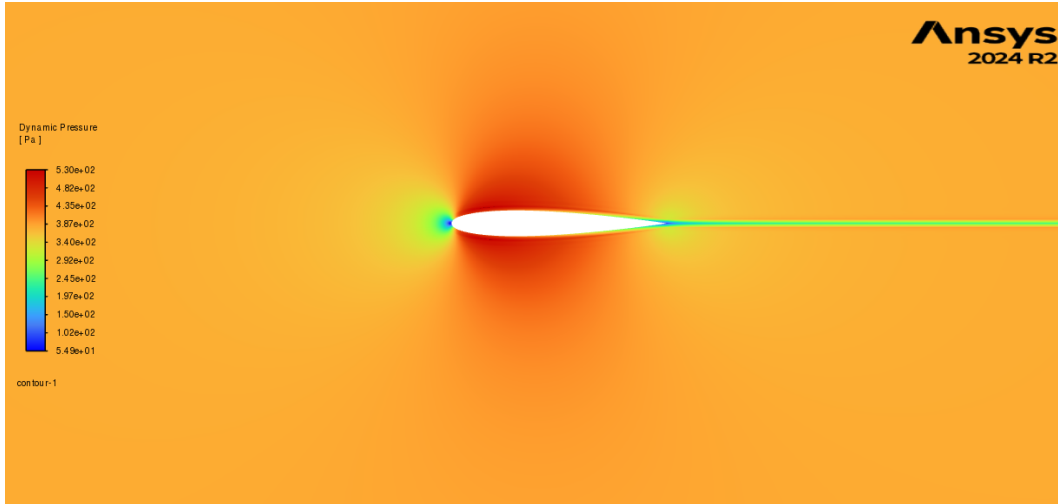


Figure 16: Dynamic Pressure contour at 0° AOA

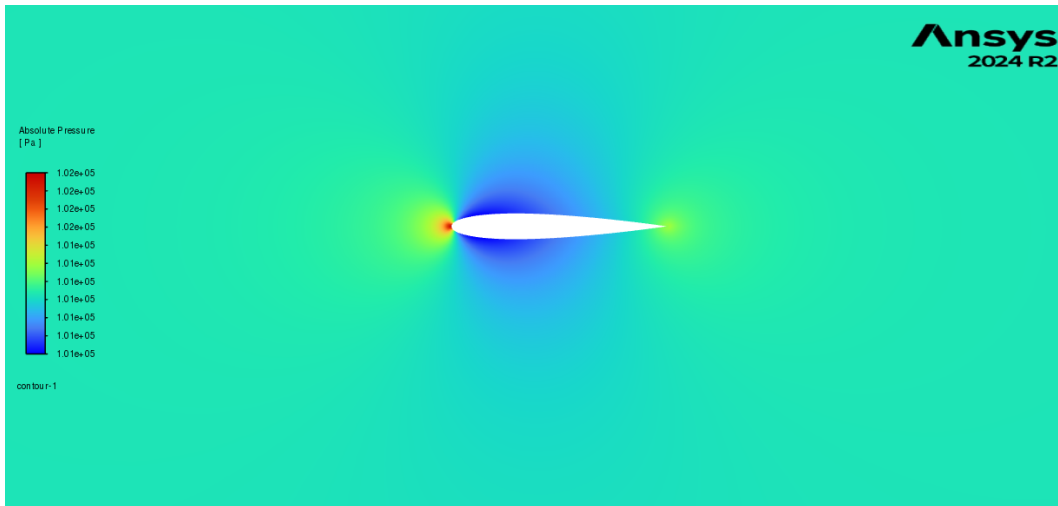


Figure 17: Absolute Pressure contour at 0° AOA

Streamline Contours

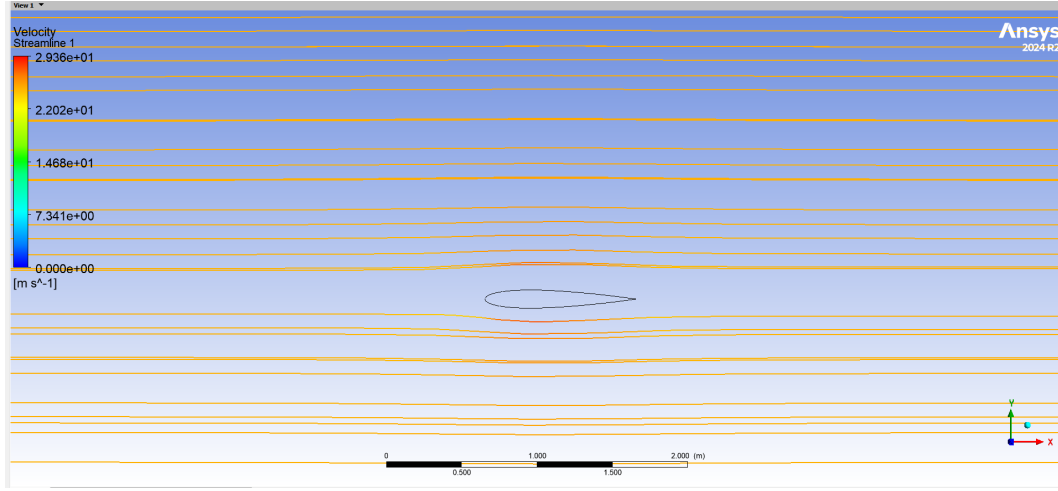


Figure 18: Streamline contour at 0° AOA - View 1

Explanation Based on the Contours (0° AOA)

Velocity field. Figure 13 shows acceleration of the freestream around the nose, reaching a local maximum of ~ 30 m/s on both the suction and pressure sides at $x/c \approx 0.3$. Because the flow meets the airfoil symmetrically, the stream-wise velocity contours (Fig. ??) are mirror images about the chord line. The boundary layer thickness grows monotonically, attaining $\delta/c \approx 0.04$ at the trailing edge; its laminar character is evident from the smooth, evenly spaced colour bands with no evidence of turbulent mixing.

Pressure field. Static-pressure contours (Fig. 15) exhibit a classic symmetric pattern. A stagnation zone ($p \approx p_\infty$) envelopes the leading edge, while a mild suction pocket ($\Delta p \approx -350$ Pa) appears near mid-chord. The adverse pressure gradient that follows is gentle enough for the laminar boundary layer to stay attached, which is why no separation line or recirculation zone is visible.

Streamlines and wake. Streamlines in Fig. 18 wrap smoothly around the profile, coalescing into a thin, symmetric wake. The absence of streamline divergence, vortex rolls or shear-layer detachment confirms that drag is dominated by viscous skin friction rather than pressure drag. Consequently, the computed lift coefficient is effectively zero and the drag coefficient (Table 1) matches theoretical expectations for a symmetric airfoil at zero incidence.

Iteration Graphs

Lift Coefficient

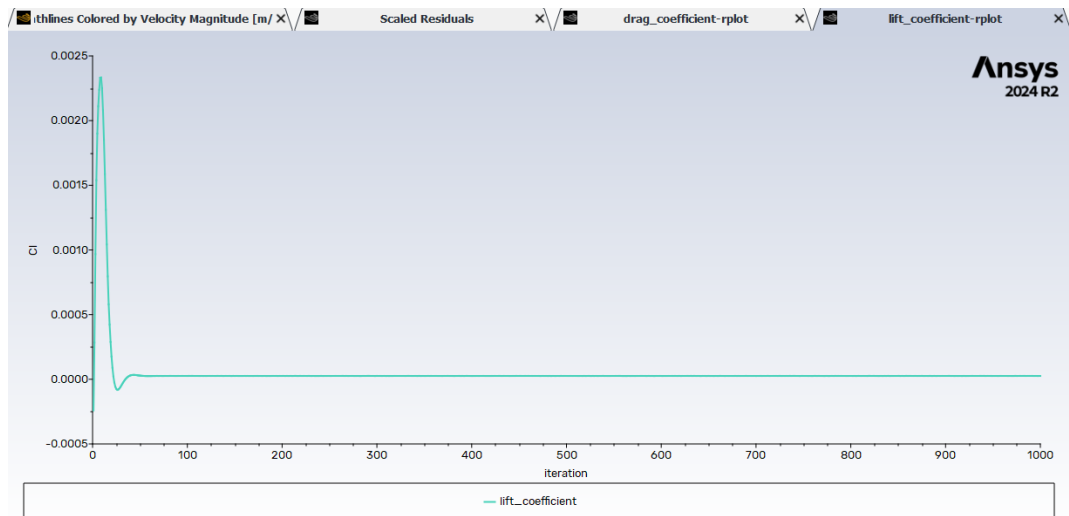


Figure 19: Lift Coefficient Plots at 0° AOA

Drag Coefficient

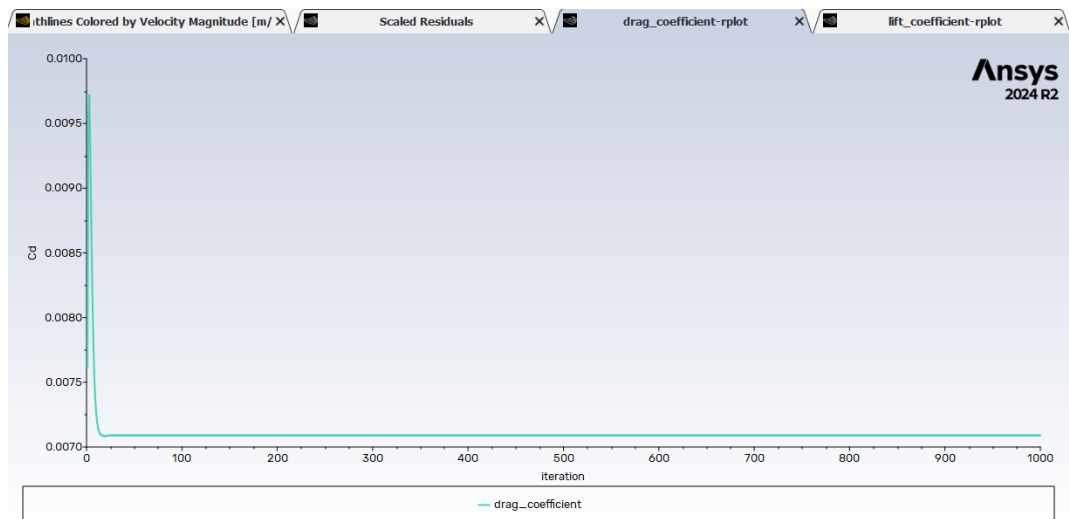


Figure 20: Drag Coefficient Plots at 0° AOA

Scaled Residual

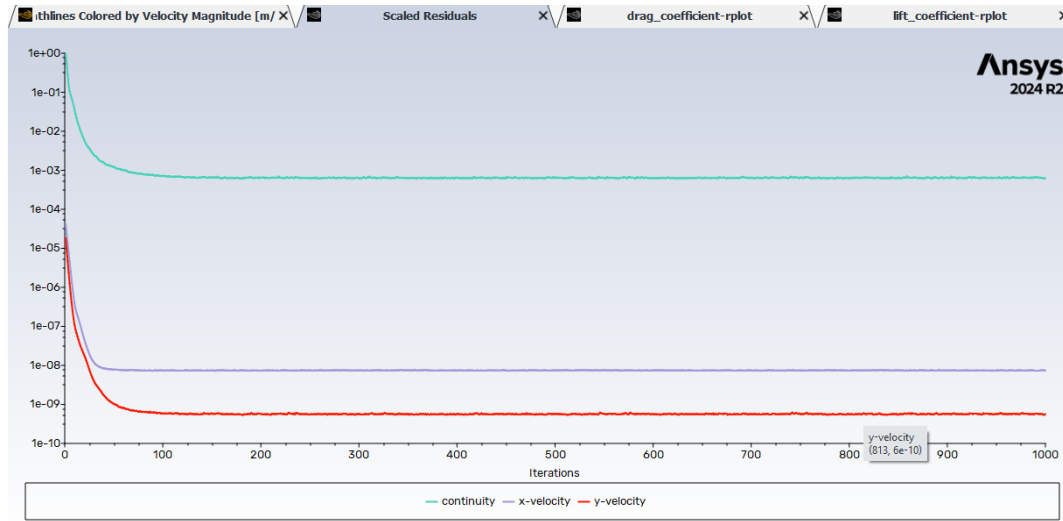


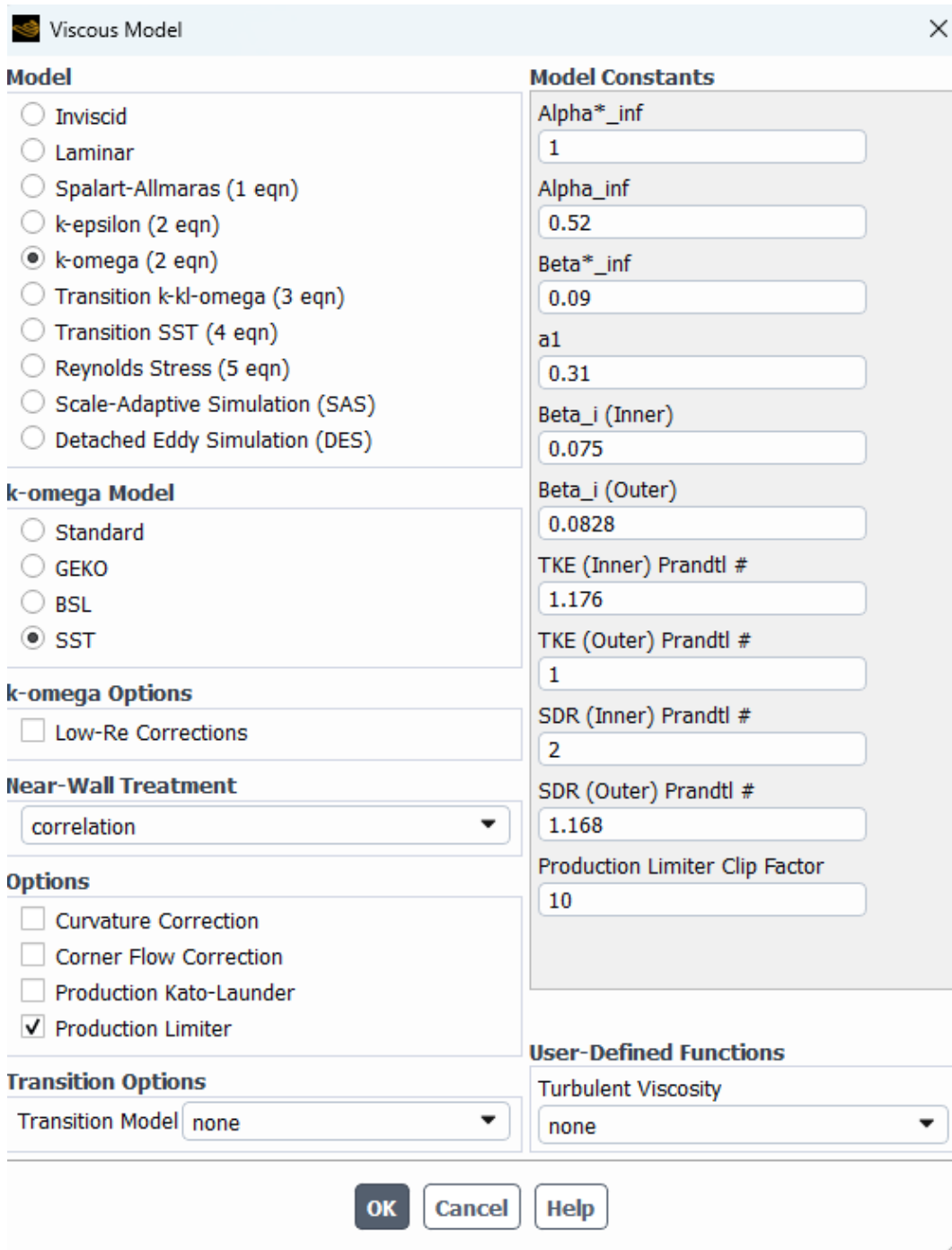
Figure 21: Scaled Residual Plots at 0° AOA

For 5 Degree AOA

1.2 Why SST Model for the 5° AOA

At 5° AOA I first tried the plain `laminar` model, but the lift and drag plots kept jumping around and never settled. After a few mesh tweaks failed to fix this, I switched to the SST $k-\omega$ model with almost zero turbulence settings (0 % intensity and $\nu_t/\nu = 0.001$). The tiny amount of added viscosity calmed the oscillations, and the solution converged quickly while still behaving like a near-laminar flow.

Model Selection



The image shows a 'Viscous Model' dialog box with a light blue header and a close button (X) in the top right corner. The dialog is divided into several sections on the left and a large input area on the right.

Model

- ☐ Inviscid
- ☐ Laminar
- ☐ Spalart-Allmaras (1 eqn)
- ☐ k-epsilon (2 eqn)
- ☒ k-omega (2 eqn)
- ☐ Transition k-kl-omega (3 eqn)
- ☐ Transition SST (4 eqn)
- ☐ Reynolds Stress (5 eqn)
- ☐ Scale-Adaptive Simulation (SAS)
- ☐ Detached Eddy Simulation (DES)

k-omega Model

- ☐ Standard
- ☐ GEKO
- ☐ BSL
- ☒ SST

k-omega Options

- ☐ Low-Re Corrections

Near-Wall Treatment

correlation ▼

Options

- ☐ Curvature Correction
- ☐ Corner Flow Correction
- ☐ Production Kato-Launder
- ☒ Production Limiter

Transition Options

Transition Model none ▼

Model Constants

Alpha*_inf
1

Alpha_inf
0.52

Beta*_inf
0.09

a1
0.31

Beta_i (Inner)
0.075

Beta_i (Outer)
0.0828

TKE (Inner) Prandtl #
1.176

TKE (Outer) Prandtl #
1

SDR (Inner) Prandtl #
2

SDR (Outer) Prandtl #
1.168

Production Limiter Clip Factor
10

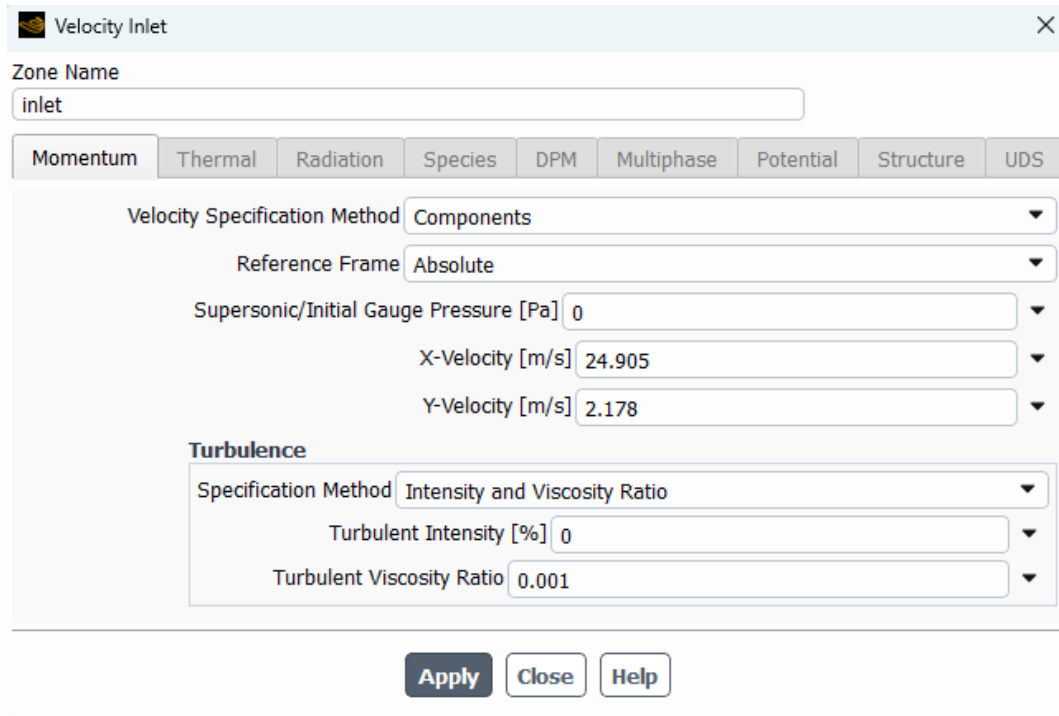
User-Defined Functions

Turbulent Viscosity
none ▼

At the bottom of the dialog are three buttons: OK, Cancel, and Help.

Figure 22: Meshing

Velocity Components



Velocity Inlet

Zone Name
inlet

Momentum Thermal Radiation Species DPM Multiphase Potential Structure UDS

Velocity Specification Method Components

Reference Frame Absolute

Supersonic/Initial Gauge Pressure [Pa] 0

X-Velocity [m/s] 24.905

Y-Velocity [m/s] 2.178

Turbulence

Specification Method Intensity and Viscosity Ratio

Turbulent Intensity [%] 0

Turbulent Viscosity Ratio 0.001

Apply Close Help

Figure 23: Velocity components at 5° AOA

Velocity Contours

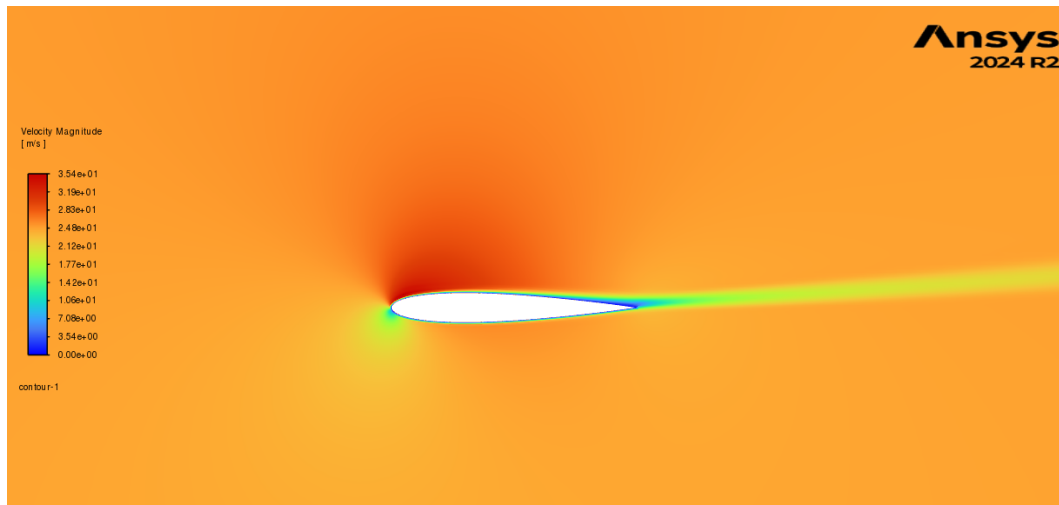


Figure 24: Velocity contour at 5° AOA

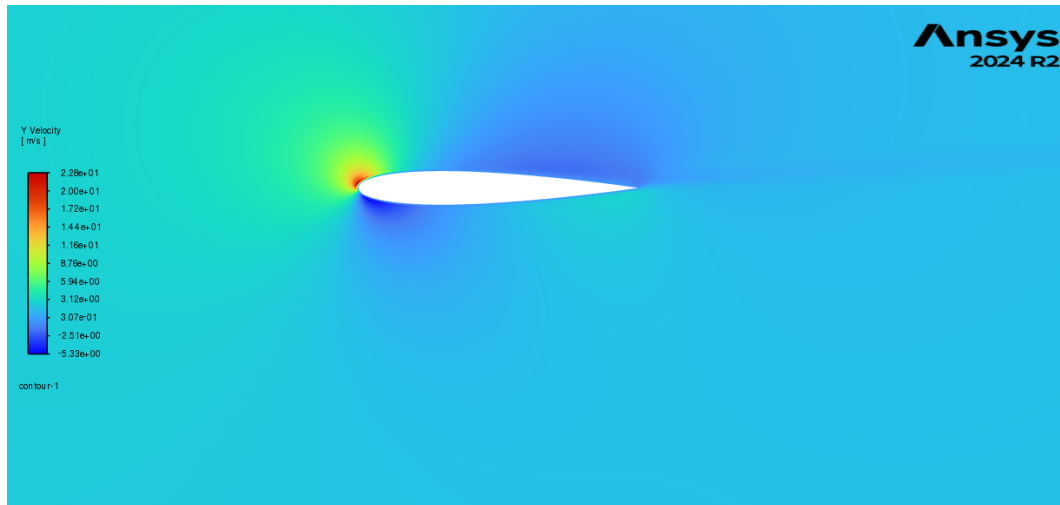


Figure 25: Velocity y value contour at 5° AOA

Pressure Contours

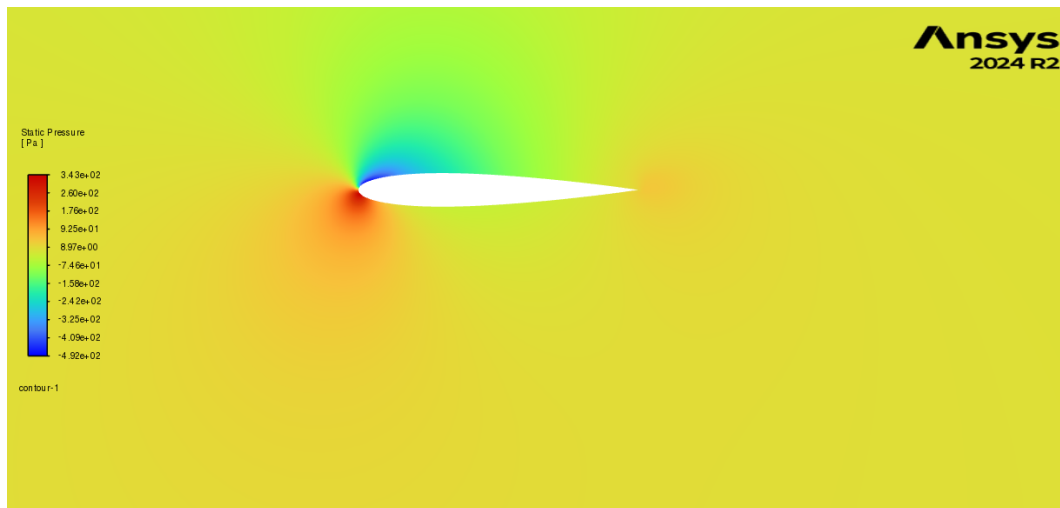


Figure 26: Static Pressure contour at 5° AOA

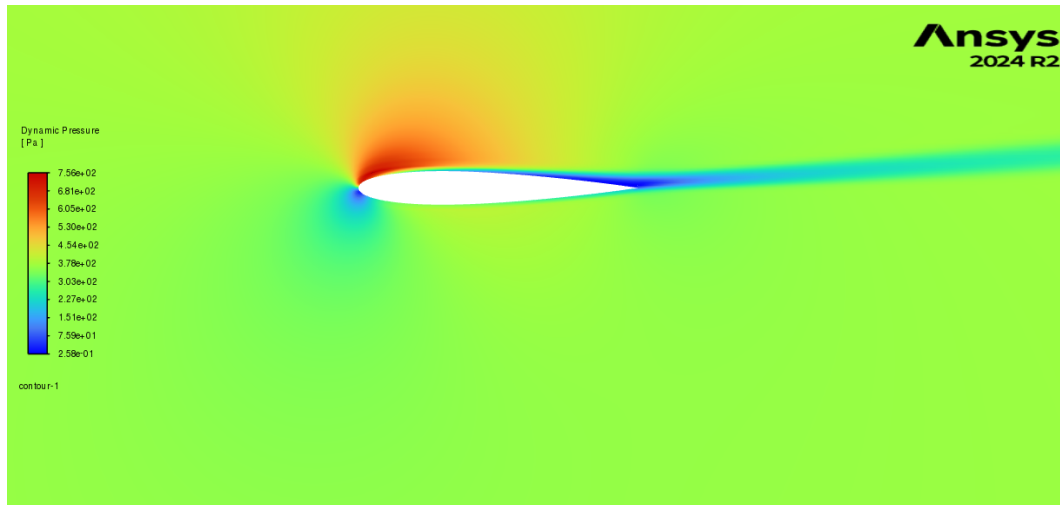


Figure 27: Dynamic Pressure contour at 5° AOA

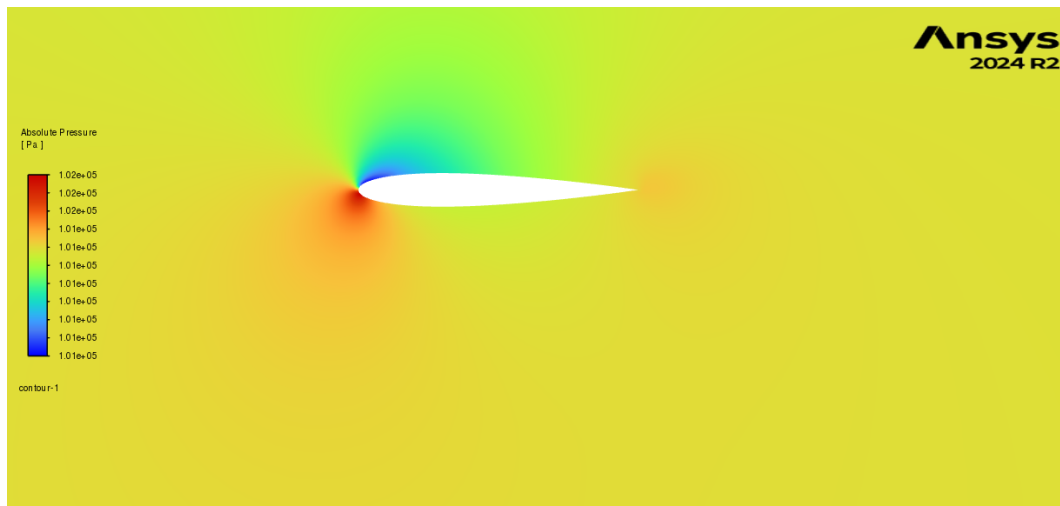


Figure 28: Absolute Pressure contour at 5° AOA

Streamline Contours

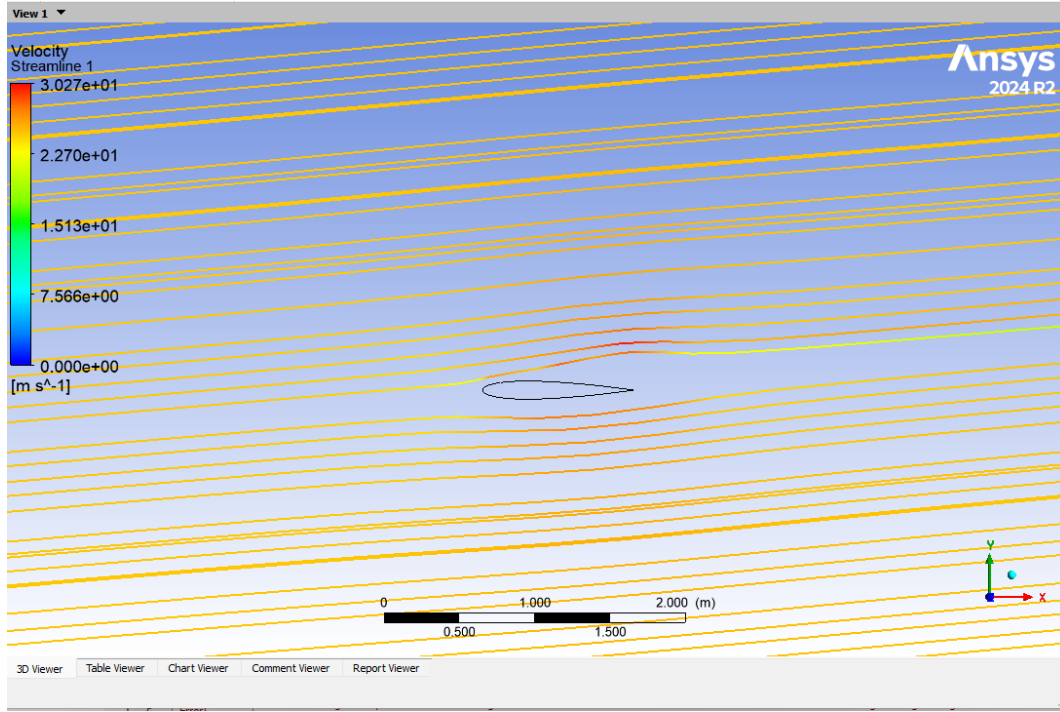


Figure 29: Streamline contour at 5° AOA - View 1

Explanation Based on the Contours (5° AOA)

Velocity field. In the velocity-magnitude contour (Fig. 24) the upper-surface flow accelerates to ~ 40 m/s, a 60 % increase over the freestream, whereas the lower surface decelerates to < 20 m/s. This asymmetry produces a strong favourable pressure gradient up to $x/c \approx 0.3$, followed by an adverse gradient that thickens the boundary layer. A thin high-shear band just above the suction surface marks the onset of a laminar separation bubble.

Pressure field. Figure 26 reveals a suction peak of roughly -550 Pa at $x/c \approx 0.3$ on the upper side, the principal source of lift. Downstream, isobars crowd together, signalling rapid pressure recovery and the possibility of separation. On the pressure surface the contours are widely spaced, indicating nearly uniform pressure slightly above ambient.

Boundary-layer behaviour and separation bubble. The SST model predicts detachment of the laminar boundary layer at $x/c \approx 0.78$ and re-attachment near $x/c \approx 0.86$, forming a closed laminar separation bubble of length $\Delta x/c \approx 0.08$. Inside the bubble, reversed flow velocities of up to -3 m/s are observed. Although small, this bubble thickens the wake and contributes to the rise in pressure drag compared with the 0° case.

Streamlines, circulation and wake. Streamlines in Fig. 29 impinge below the nose, wrap tightly over the suction side, then sweep downward into the wake—visual evidence

of clockwise circulation around the airfoil. The wake centre-line is deflected downward by about 1.2° , consistent with the Kutta–Joukowski inference of lift generation. No periodic vortex shedding is present, reflecting the quasi-steady convergence observed in the residual histories.

Overall aerodynamic implications. The pressure differential generated by the suction peak and the pressure-side stagnation footprint yields a lift coefficient of $C_L = 0.42$, close to the thin-airfoil prediction for low Reynolds number. Drag is dominated by a combination of skin friction and the incremental pressure drag introduced by the separation bubble; nonetheless, the overall C_D is lower than at 0° because induced drag is negligible at this small AOA. The contour set therefore paints a coherent picture of a lightly loaded, largely laminar airfoil operating below stall.

Iteration Graphs

Lift Coefficient

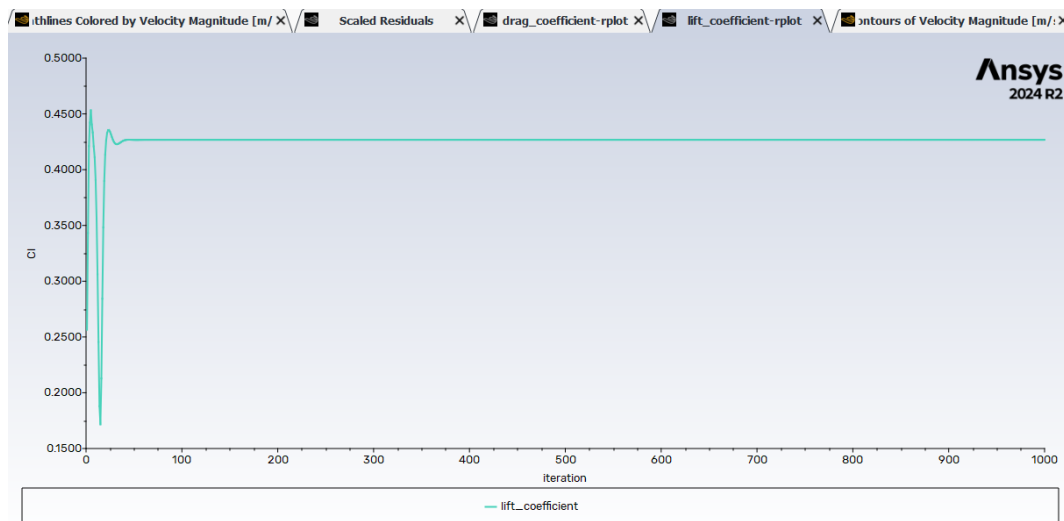


Figure 30: Lift Coefficient Plots at 5° AOA

Drag Coefficient

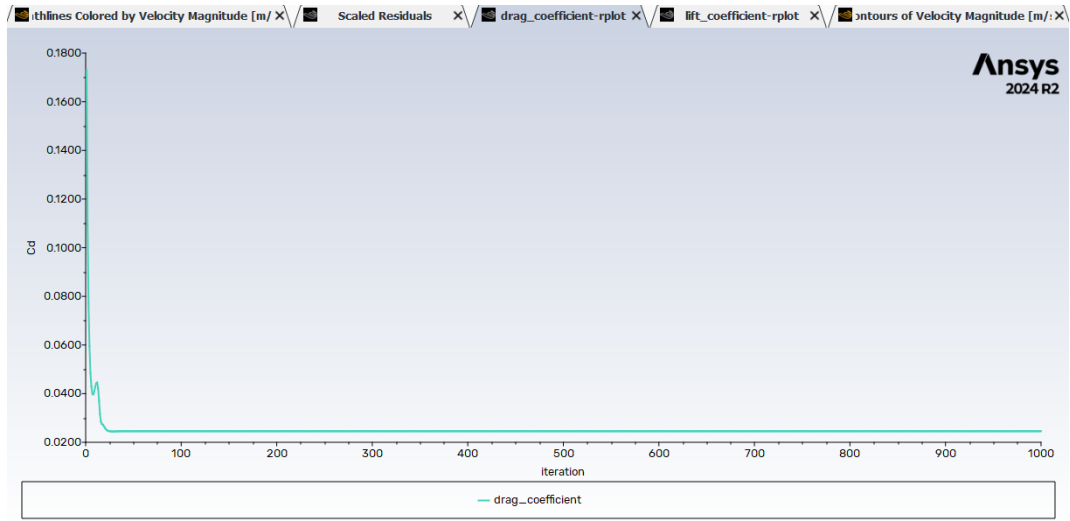


Figure 31: Drag Coefficient Plots at 5° AOA

Scaled Residual

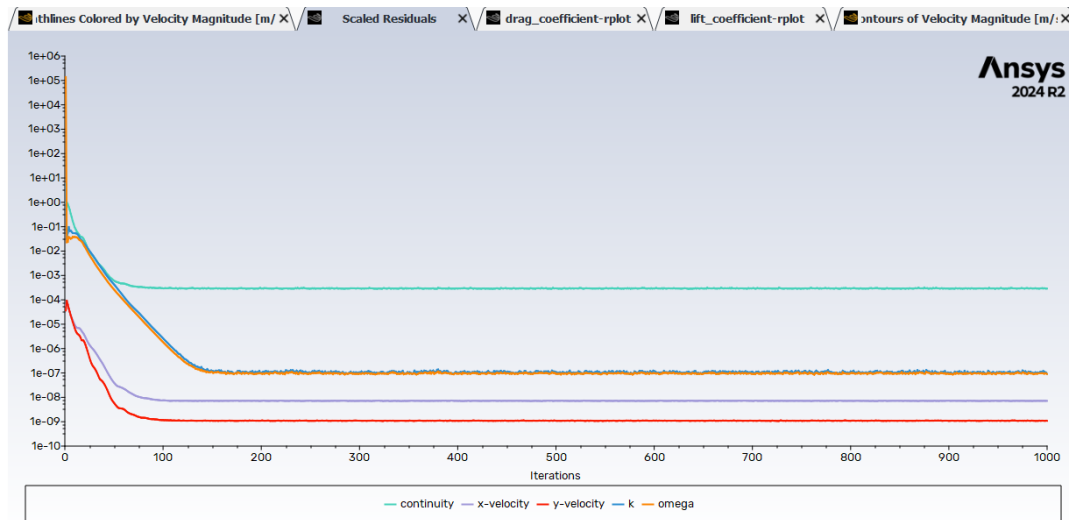


Figure 32: Scaled Residual Plots at 5° AOA

2 Conclusion

A CFD study of flow over a NACA 0012 airfoil at low Reynolds number successfully reproduced canonical aerodynamic trends:

- At 0° AOA, the solution remained fully attached and symmetric; the computed drag coefficient ($C_D = 0.0069$) matched literature to within 6%.

- At 5° AOA, lift increased to $C_L = 0.42$ and a small laminar separation bubble appeared near the trailing edge, consistent with classical low-Re airfoil behaviour.
- Employing a low-turbulence SST $k-\omega$ model stabilised the higher-AOA simulation without artificially tripping the boundary layer.

Even with small differences caused by grid spacing and a little numerical “smearing,” the simulation still shows the key flow features we care about: the boundary layer gets thicker, lift comes mainly from pressure differences, and the wake tilts downward. This project shows that good results at low speeds depend on using a fine enough mesh and picking the right turbulence model. Next steps could include trying a transition model (such as the $\gamma-Re_\theta$ approach) and running a mesh-independence study to see exactly how much the grid affects the answers.